Microgravity Science and Technology

Characterization of the accelerometric environment of DCMIX2/3 experiments

--Manuscript Draft--

Manuscript Number:	
Full Title:	Characterization of the accelerometric environment of DCMIX2/3 experiments
Article Type:	ELGRA2017
Keywords:	DCMIX experiment; ISS acceleration signal; ISS vibrational environment; spectral entropy; linear correlation between ISS acceleration signals
Corresponding Author:	Fina Gavaldà, PhD Universitat Rovira i Virgili Tarragona, Tarragona SPAIN
Corresponding Author Secondary Information:	
Corresponding Author's Institution:	Universitat Rovira i Virgili
Corresponding Author's Secondary Institution:	
First Author:	Diana Dubert, PhD
First Author Secondary Information:	
Order of Authors:	Diana Dubert, PhD
	Judit Ollé, M.D.
	Rafael Jurado, M.D.
	Fina Gavaldà, PhD
	Ana Laverón-Simavilla, PhD
	Xavier Ruiz, PhD
	Valentina Shevtsova, PhD
Order of Authors Secondary Information:	
Funding Information:	Ministerio de Economía y Competitividad (ESP2014-53603-P) — Professor Xavier Ruiz
Abstract:	This work presents a comparative analysis of the vibratory environment during DCMIX2/3 thermodiffusion experiments by using acceleration signals coming from different sensors placed in the Destiny, Columbus and Kibo modules. The es03 sensor located inside the Glovebox, nearest to the experimental device, has been selected as reference. Data were downloaded from the NASA PIMS website paying special attention to the runs coinciding with disturbances such as dockings or Extra Vehicular Activities (EVAs), as they could particularly affect the International Space Station, ISS, microgravity levels. The analysis has been made minute by minute by using specific mathematical manipulations, such as: the Frequency Factor Index (FFI), the Spectral Entropy (SEN) and the Root Mean Square (RMS) values evaluated over one-third-octave frequency bands. Spearman's rank correlation coefficient and the coherence function has also been used to investigate the degree of correlation of the signals with the reference one. SEN evolution associated to the acceleration components showed different patterns compared to the reference. RMS values that surpassing the ISS microgravity conditions were detected in all sensors, mainly at low frequency bands (<10 Hz), prevailing on zA direction. The es03 reference sensor respected better the ISS vibratory limits requirements. Some degree of linear correlation at low frequencies (< 3 Hz - structural range) has been detected. Overall, the sensors placed in the Destiny, Columbus and Kibo modules presented different vibratory characteristics and, despite they offer valuable information of the whole environment, are not enough to properly characterize any DCMIX2/3

	experiments.

Characterization of the accelerometric environment of DCMIX2/3 experiments

D. Dubert[a], J. Ollé[a], R. Jurado[a], Jna. Gavaldà[a*], A. Laverón-Simavilla[b], X. Ruiz[a,c], V. Shevtsova[d]

[a] Departament Química Física i Inorgànica, Universitat Rovira i Virgili. Tarragona, Spain.
[b] E-USOC. ETSIAE, Universidad Politécnica de Madrid. Madrid. Spain.
[c] Institut d'Estudis Espacials de Catalunya, IEEC. Barcelona. Spain.
[d]Department of Chemical Physics, MRC, Université Libre Bruxelles, Belgium.
*Corresponding author: fina.gavalda@urv.cat

Abstract

This work presents a comparative analysis of the vibratory environment during DCMIX2/3 thermodiffusion experiments by using acceleration signals coming from different sensors placed in the Destiny, Columbus and Kibo modules. The es03 sensor located inside the Glovebox, nearest to the experimental device, has been selected as reference. Data were downloaded from the NASA PIMS website paying special attention to the runs coinciding with disturbances such as dockings or Extra Vehicular Activities (EVAs), as they could particularly affect the International Space Station, ISS, microgravity levels.
The analysis has been made minute by minute by using specific mathematical manipulations, such as: the Frequency Factor Index (FFI), the Spectral Entropy (SEN) and the Root Mean Square (RMS) values evaluated over one-third-octave frequency bands. Spearman's rank correlation coefficient and the coherence function has also been used to investigate the degree of correlation of the signals with the reference one. SEN evolution associated to the acceleration components showed different patterns compared to the reference. RMS values that surpassing the ISS microgravity conditions were detected in all sensors, mainly at low frequency bands (<10 Hz), prevailing on z_A direction. The es03 reference sensor respected better the ISS vibratory limits requirements. Some degree of linear correlation at low frequencies (< 3 Hz - structural range) has been detected.
Overall, the sensors placed in the Destiny, Columbus and Kibo modules presented different vibratory characteristics and, despite they offer valuable information of the whole environment, are not enough to properly characterize any DCMIX2/3 experiments.

Keywords: DCMIX experiment; ISS acceleration signal; ISS vibrational environment; spectral entropy; linear correlation between ISS acceleration signals

1. Introduction

To have an accurate accelerometric characterization of any experiment carried out in the International Space Station (ISS), the use of data coming from an onsite sensor, nearest to the experimental device, should be the common choice. Though, frequently, and for different reasons, this is impossible and the characterization must be made based on data provided by other sensors located far from the experimental equipment either in the same module or in a different module of the Station. In this situation, an evident question, related with the reliability of the conclusions, arises (Sáez et al. 2014). The present work discusses this relevant point in the frame of the DCMIX2/3 thermodiffusion experiments (Lappa et al. 2012; Mialdun et al. 2013a,b, 2015; Shevtsova et al. 2014; Mezquia et al. 2015; Jurado et al. 2016; Bataller et al. 2016; Santos et al. 2016). The characterization of the onsite acceleration environment of both experiments has been reported in a recent study (Ollé et al. 2017), by using the es03 sensor, located in the Microgravity Science Glovebox (MSG) inside the Destiny module, as reference. Herein, data coming from different sensors placed in the Destiny, Columbus and Kibo modules were also used to study the whole accelerometric environment. Due to the lack of acceleration data, not all the runs have been able to be globally considered. In order to analyze the worst possible scenario, signals coinciding with the occurrence of potentially dangerous external disturbances such as reboosting, dockings or EVAs have particularly been studied. Furthermore, to be as exhaustive as possible, a run during a quiescent period was also included for each DCMIX2 and DCMIX3 experiments.

As a consequence of this study, the degree of reliability of the information derived from the comparative analysis of the different acceleration data coming from the different sensors was discussed. Then, the usefulness of the accelerometric environmental information (the use of distant sensors) to characterize a specific experiment was also carefully considered.

2. Numerical procedures

2.1. Sensor details

The signals analyzed in the present article are summarized in Table 1. Runs 1b and 16 correspond to DCMIX2 experiment and Runs 6 and 20a belong to DCMIX3. Run 16 (October 26th of the 2013) was performed coinciding with an Extra Vehicular activity (EVA), while Run 1b (10th December of 2013) was selected due to the good quality of the microgravity environment (quiescent). In case of DCMIX3, Run 20a coincided with a docking event (21st October of 2016), and as a quiescent period, Run 6, occurred on the 27th September of 2016. The sensors used to generate DCMIX2/3 signals were: es03, 121f03, 121f08 and 121f05, thereafter S1, S2, S3 and S4, respectively. The first two were located inside the Destiny module, while the last two ones were placed in the Columbus and Kibo modules, respectively. Details of their specific position and characteristics are presented in Table 2. Notice that, during the Run 16 (DCMIX2), Columbus and Kibo sensors were inoperative.

All signals have been downloaded from NASA Principal Investigator Microgravity Services (PIMS) website as binary files (PIMS website: PIMS 2018). Data units are in g (9.8m/s^2) and before any mathematical manipulation, all raw signals have been systematically demeaned. The acceleration components always refer to the absolute coordinates of the International Space Station (Jules 2006)**Error! Reference source not found.**. As mentioned elsewhere (Ollé et al. 2017), to accurately detect possible oscillatory disturbances during the DCMIX2/3 experiments, the signals were segmented in k records of 1 minute each.

2.2. Mathematical characterization

The one-minute interval root-mean-square (RMS) together with the spectral entropy magnitude have been estimated for each acceleration component (Ollé et al. 2017). The calculation of the Spectral Entropy magnitude, SEN, is based on the power spectrum density (PSD) as follows:

$$SEN = -\frac{\sum_f P_f\,(log P_f)}{\log(N)} \quad (1)$$

where N is the number of discrete frequencies and P_f is the normalized PSD of each acceleration component with a spectral content below a predefined maximum frequency value.

Herein, were selected two maximum values, 20 Hz (low frequency interval) and the cut-off frequency (whole frequency interval) (Shannon 1948). The particular interest in the low frequency interval (f < 20 Hz) is due to their potential perturbative impact in liquid systems as the thermodiffusive ones (Yan et al. 2005). Notice also that a particular advantage of using the spectral entropy as a signal disturbance indicator is that the contributions of different frequency bands could be explicitly considered with the aim of observing their specific changes.

In a previous work (Ollé et al.2017), the existence of a good correlation between the RMS spikes and the SEN peaks was confirmed if the whole frequency interval was considered (see Fig 1). Due to this, the SEN magnitude was used as a warning parameter to detect possible disturbances during any run.

The frequency factor index (FFI) was considered for low frequency intervals in order to condense into one figure the global relevance of the corresponding interval. The definition of this scalar, for one record k, is as follows

$$FFI(f)_k = log\frac{Max(PSD_k)}{PSD_k(f)} \quad (2)$$

where $PSD_k(f)$ means the relative maximum magnitude of the PSD for a specific frequency interval and $Max(PSD_k)$ represents the absolute maximum value for all the frequency range. Two intervals were chosen considering only the low frequency ranges, 20 Hz and 1 Hz, respectively.

Based on the PSD evaluation and using the Parseval theorem, the one-min RMS levels, integrated over each one of the one-third octave bands below the cutoff frequency, were also calculated for each component of acceleration (Hrovat 2004; Rogers et al. 1997). These RMS levels were compared minute by minute to the standard curve defining the NASA's ISS vibratory limit requirements (DeLombard et al. 2005; Jules et al. 2004a).

Correlations between the acceleration components coming from the different sensors against the reference one, have also been investigated. Calculations have been restricted to the components acting only in the same direction: a_x(S*) - a_x(S1), a_y(S*) - a_y(S1) and a_z(S*) - a_z(S1), where "*" indicates the rest of the sensors (2, 3, 4). From a quantitative point of view and due to the non-Gaussian character of the signals involved (details about the uni/bimodality, skewness and kurtosis of all signals are presented in Table 3) the selected correlator was the Spearman's rank correlation coefficient (Hinkle et al. 2003) defined as:

$$r_s = 1 - \frac{6\sum_{i=1}^{N} di^2}{N(N^2-1)} \quad (3)$$

where di is the difference in ranks of the two acceleration components and N represents the number of data used.

Needless to say, this nonparametric version of the Pearson correlation indicates how well the relationship between two signals can be described using a monotonic function. The r_s value is bounded by ±1, and is not affected by the existence of outliers which may exaggerate or damp the strength of the relationship (as in case of Pearson). Calculations about the percentage of outliers of each signal have been estimated based on the Tuckey's method (Seo 2006) (see Table 3).

In the frequency domain, the linear dependency between couples of acceleration components was investigated considering the calculated coherence magnitude values (Bendat et al. 2010). The well known mathematical expression of the coherence, C_{xy}(f), is based on power spectral estimations as follows:

$$C_{xy}(f) = \frac{|P_{xy}(f)|^2}{P_{xx}(f)\ x\ P_{yy}(f)} \quad (4)$$

where P_{xx}(f) is the power spectrum of the first signal, P_{yy}(f) is power spectrum of the second one and P_{xy}(f) is the cross power spectrum of both signals. The coherence ranging between 0 and 1, indicates how well the two signals relate to each other at a certain frequency (Bendat et al. 2010). In other words, zero coherence value indicates that the two signals have no linear correlation at this frequency, while a value of one indicates a complete linear correlation at the specified frequency. Due to the difference in sampling rate of S1 sensor compared to the others, a re-sampling of all signals at 250 Hz was needed, in order to obtain the coherence values.

3. Results and discussion

3.1. Spectral entropy analyses

Figs. 2.a and 2.b display the minute by minute SEN values for two different sensors, S1 and S2 respectively, during the Run 16 of the DCMIX 2 experiment. The rectangle in both figures indicates the time period corresponding to the Extra Vehicular Activity (EVA). The SEN values associated to the three acceleration components are plotted for both the low and the whole frequency ranges. In case of the S1 sensor (see Fig. 2.a), SEN values, calculated for the whole interval of frequencies, present some spikes at the end of the run (approximately after 20h of experiment) for the three coordinates corresponding to the EVA disturbance period. Due to the absence of this spikes in the SEN evolution of the S2 sensor (Fig. 2.b), it cannot be assured that the above-mentioned disturbance was the direct responsible for the S1 behavior. In addition, the SEN associated with the a_y and a_z components, presents a higher degree of oscillation compared to the other one (a_x). The S2 SEN values show a more stabilized evolution all along the run.
Fig. 3 displays the SEN evolution, calculated for the whole interval of frequencies, of the three acceleration components for Run 6, corresponding to a quiescent period of the DCMIX2 experiment, for the four sensors considered. Notice that the signal coming from S1 sensor lasted 20 hours approximately due to lack of data. The sensor that presents more spikes is S1. These spikes are more pronounced in the y_A-z_A plane. As the above spikes are present only in the SEN values related with whole frequency interval, they could probably be the result of the running machinery (high frequencies) inside the Glovebox (Jules et al. 2004b). The SEN values for the other three sensors, show a more stable evolution all along the experiment.
SEN analyses were, as well, applied for the signals recorded during the DCMIX3 experiment (see Figs. 4 and 5). Fig. 4 corresponds to Run 20a and the rectangle shows the Soyuz docking period between the 9 and 13 hours of the run. During the 22 hours of experiment, the SEN values were practically constant at all times for all the signals and all three coordinates, except for the one generated by S3 sensor, which presented different periods with significant spikes and oscillations in all directions (x_A, y_A, z_A), mainly if the entire range of frequencies was considered (see Fig. 4.c). The first period with the sharpest spikes, corresponding to the period when the docking occurred, is more pronounced in the z_A direction. This direction coincides with that of the external disturbance (See Table 1). The second spiky period detected at the end of the run, has an unknown source. In case of the S2 sensor (see Fig. 4.b), some small oscillation could also be appreciated during the period matching with the docking event. This situation is not reproduced in the other sensors (see Fig. 4.a and d). Analyzing the signals coming from the four selected sensors during Run 6, (see Fig. 5), a very similar behavior in the SEN values is observed for both frequency intervals and for the three components. There is, though, a small difference in the degree of oscillation, when sensor S3 and the whole range of frequency are considered. In particular, intense spikes were detected along the 22 hours of run mainly in the z_A direction. In other

words, the sensor located in the Columbus module always shows high sensibility to vibratory environment compared to the other modules.
During both DCMIX2/3 experiments, S1 sensor showed different patterns compared to the S3 and S4 ones, located in the Columbus and Kibo modules, respectively. However, some similarities have been detected between S1 and S2 sensors, both placed in the same module. Moreover, the slight differences in patterns of same sensors (S1 and S3 sensors) during DCMIX 2/ 3 experiments, might be due to their different location (See Table 2). This suggests that the position of the sensors within the modules has a great importance.
In summary, Figs. 2, 3, 4 and 5 confirm the utility of the Shannon entropy as a fast and robust indicator for the detection of possible disturbances in time when the whole frequency range is used.

3.2. Frequency Factor Index analyses

Table 4 presents the values of the FFI for both DCMIX2/3 experiments including all the active sensors in each run. The table also includes the frequencies related to the absolute maxima of the power spectrum and its magnitude. Usually, the FFI values are similar for the three components of the same sensor, while are distinct for different sensors. Nevertheless, taking into account the maximum frequency elected for each case and its PSD intensity and by using the equation 2, the PSD intensities associated to the specified intervals (< 1 Hz and < 20 Hz) become similar.
Moreover, the FFI values obtained at frequencies less than 1 Hz, usually, show higher values than the ones calculated for the 20 Hz interval. In general, a high FFI value is a good indication of the small percentage of power associated to low frequencies ranges, the most damaging in thermodiffusion experiments. Furthermore, Table 4, shows that the frequency associated to the maximum PSD, changes with the direction and with the sensor selected. In order to explain a possible origin of the different main frequencies detected by the sensors, Table 5 summarizes the main spectral fingerprints of different mechanical disturbances compiled from the NASA PIMS Microgravity Environment Handbook (Jules et al. 2004b; McPherson et al. 2015; NASA PIMS Handbook 2013). Remark that, the 73.1 Hz frequency is detected as dominant frequency for the signals coming from S1 sensor located in the MSG and for the three components. According to the Table 4, this peak can be attributed to the MSG fan in open mode. In the case of the others sensors, high frequencies, between 50-100 Hz, govern the power distribution and might thus be linked to general machinery functioning.

3.3. Root Mean Square obtained by integration over each one of the different one-third-octave frequency bands

It has been demonstrated (Ollé et al. 2017) that the minute by minute RMS acceleration values expressed in one third octave frequency band, that overcome the ISS limit requirements in the vibratory range, may be successfully plotted as visual warnings. Figs. 6, 7, 8 and 9 present the RMS warning maps applied for the signals considered herein.

In case of DCMIX2 experiments, for both runs and for the sensors selected (See Figs. 6 and 7), the microgravity mode condition is accomplished for frequencies above 10 Hz, except some warnings detected for the S1 sensor, Run 16, in the z_A direction. Note that at smaller frequencies the limit is surpassed during most of the duration of the experiment. These warnings detected during the experiment do not increase during the EVA period (see Fig. 6 - rectangle). Comparing the signals during the quiescent period (see Fig.7) the sensors located in Columbus and Kibo modules, were more affected by vibrations, especially considering the low frequency range (less than 10 Hz) and z_A direction.

Analyzing DCMIX3 experiments, Figs. 8 and 9, it can be seen that two of the sensors (S4 and S3) showed no warning for frequencies above 10 Hz, meanwhile the other two (S2 and S1) surpassed the ISS limit at higher frequencies, especially for the z_A direction. This fact is accentuated for S2 sensor around the frequencies 40 and 66 Hz. According to the Table 4, the source of these particular frequencies might be the internal thermal control system equipment. Taking into account the low frequency range, the sensors placed in Columbus and Kibo modules, are more sensitive to the vibrations compared to the other two sensors, especially in the z_A direction. This fact is valid considering both the docking and quiescent periods. Focusing on the docking period, Fig. 8, black rectangle, non-visible increment of warnings, due to this, has been detected.

The visual warning map tool enables an easier and faster identification of the points in time and frequency that outdo the ISS limit requirements for a better monitoring of the possible dangerous disturbances that might have a great effect on the ongoing experiments.

3.4. Spearman and coherence analyses

In order to study the relationship between same acceleration components of the reference S1 with other sensor, the Spearman coefficient and the coherence magnitude have been applied. As an example, Figs. 10.a and b present the scatterplots and Spearman coefficients for both experiments: DCMIX2, Run 16 (EVA period) and DCMIX3, Run 20a, docking period, respectively. These plots correspond to the S1 (reference) and the S2 sensors for the same a_z acceleration component. The scatterplots (Figs. 10.a1 and b1) have been used with the aim of rapidly visualize the signal’s tendency, herein inexistent in both cases. The values of the Spearman

coefficients, Figs. 10.b1 and b2, confirm this point. Appreciably the presence of the great number of outliers, detected in both cases (see Table 3).
As specified earlier, coherence analysis helps to have a quick overview of the linear correlation at specific frequencies between the different sensors. As an example of the results found, Fig. 11.a. plots the coherence values calculated between S1 and S2 sensors, for Run16 (DCMIX2). The coherence magnitude computed between S1 and the other three sensors is presented in Figs. 11.b, c and d, for the Run 20a (DCMIX3). At first glance, noticeable coherence values at low frequencies (< 3Hz, see Fig. 11's detailed magnification in Fig. 12), between the signals, in all three direction and both runs have been found. For higher frequencies this magnitude tends to zero. This fact suggests that the mechanical couplings between modules are partially linear only for low and very low frequencies, known as structural ones (McPherson et al. 2015). Similar tendency was found comparing coherence values for the three spatial directions. A partial linear association in S2 and S4 sensors was also detected around the 23 Hz, coinciding with the Russian SKV air conditioner.

4. Conclusions

A detailed and comparative analysis of the vibratory environment of the DCMIX2/3 experiments were carried out minute by minute using acceleration signals coming from Destiny, Columbus and Kibo modules. The results obtained have been compared with the reference sensor.
The SEN technique was used to study the regularity of the power distribution in time for a specific signal. This allowed to detect the main spikes during the experiments which correlated perfectly with RMS results presented elsewhere (Ollé et al. 2017). Depending on the selected sensor the main disturbances occurred during the runs, could be detected or not. Weak disturbances as, extra vehicular activity, EVA, may be distinguished in SEN values inside the MSG for the three directions while in other locations of the ISS it was undetected. Strong disturbances as docking, have been clearly identify in the Columbus module and were inappreciable with the other sensors. In general, the Columbus module presented higher SEN spikes being more vulnerable to the vibrations.
The FFI value was used to quantify the PSD intensity in two low frequency ranges (< 1Hz and < 20 Hz). Comparing the FFI values between all sensors, for both experiments, one could detect differences between the values, though considering the maximum frequency and its intensity, the absolute PSD intensities in the low frequency bands become similar. This indicates little influence of the above frequencies on the ongoing thermodiffusive experiments.
The new RMS warning map tool has been able to identify if microgravity mode conditions were accomplished or not. On one hand, RMS warning map detected predominant disturbances on z_A direction at low frequency bands, <10 Hz for all sensors. On the other hand, the sensor located inside the MSG showed less sensitivity to vibrations compared to Columbus and Kibo ones.

Correlation analyses based on the coherence function to detect linear associations between all signals, indicated partial correlation only when low frequencies (< 3Hz) were considered.

Based on the above results it can be concluded that the sensors placed in the Destiny, Columbus and Kibo modules presented different vibratory characteristics and, despite they offer valuable information of the whole environment, are not useful enough to properly characterize the DCMIX2/3 experiments. The most appropriate accelerometric information was given by the onsite sensor.

Acknowledgments

We acknowledge the constant support offered by Dr. K. Hrovat (ZIN Technologies, Inc.). This work was supported by the Spanish Ministerio de Economia y Competitividad, MINECO, grant number ESP2014-53603-P

References

Bataller, H., Giraudet, C., Croccolo, F., Ortiz de Zarate, J.M.: Analysis of non-equilibrium fluctuations in a ternary liquid mixture. Microgravity Sci. Technol. 28: 611 (2016)

Bendat, J. S., Piersol, A. G.: Random Data: Analysis and Measurement Procedures. Fourth ed., John Wiley & Sons, Inc., Hoboken, NJ, USA (2010)

DeLombard, R., Hrovat, K., Kelly, E., Humphreys, B.: Interpreting the international Space station microgravity environment, in: Proceedings of the 43rd AIAA Aerospace Sciences Meeting and Exhibit (ASME). Reno, Nevada, U.S.A (2005) (AIAA-2005-0727)

Hinkle, D. E., Wiersma, W., Jurs, S. G.: Applied statistics for the behavioral sciences. Fifth ed., Houghton Mifflin, Boston (2003)

Hrovat, K.: Analysis Techniques for Vibratory Data, NASA 7th Annual Microgravity Environment Interpretation Tutorial. NASA Glenn Research Center. Ohio Aerospace Institute. Cleveland, Ohio, (2004)

Jules, K., McPerson, K., Hrovat, K., Kelly, E., Reckart, T.: A status report on the characterization of the microgravity environment of the International Space Station. Acta Astronaut. 55, 335–364 (2004a)

Jules, K., McPerson, K., Hrovat, K., Kelly, E.: Initial characterization of the microgravity environment of the international space station: increments 2 through 4. Acta Astronaut. 55, 855-887 (2004b)

Jules, K.: International Space Station Increment 6/8 Microgravity Environment Summary report. Nasa Technical report Server. https://ntrs.nasa.gov/search.jsp?R=20060012257 (2006). Accessed 31January 2018

Jurado, R., Gavaldà, Jna., Simón, M.J., Pallarés, J., Laverón-Simavilla, A., Ruiz, X., Shevtsova, V.: Some considerations on the vibrational environment of the DSC-DCMIX1 experiment onboard ISS. Acta Astronaut. 129, 345-356 (2016)

Lappa, M., Piccolo, C., Esposito, G., La Gala, S., Sorrentino, D., Giordano, D., De Chiara, G., Di Constanzo, G., Fortezza, R., Albanese, C.: The SODI diffusion Soret Coefficient experiment onboard ISS: a flexible and modular approach to operations in orbit, in: Proceedings of the 63rd IAF International Astronautical Congress, Naples, Italy (2012)

McPherson, K., Hrovat, K., Kelly, E., Keller, J.: A Researcher's Guide to: International Space Station Acceleration Environment, NASA Report NP-2015-11-040-JSC (2015)

Mezquia, D.A., Larranaga, M., Bou-Ali, M.M., Madariaga, J.A., Santamaría, C., Platten, J.K.: Contribution to thermodiffusion coefficients measurements in DCMIX Project. Int. J. Therm. Sci. 92, 14–16 (2015)

Mialdun, A., Shevtsova, V.: Communication: new approach for analysis of thermodiffusion coefficients in ternary mixtures. J. Chem. Phys. 138, 161102 (2013a)

Mialdun, A., Minetti, C., Gaponenko, Y., Shevtsova, V., Dubois, F.: Analysis of the Thermal Performance of SODI Instrument for DCMIX Configuration. Microgravity Sci. Technol. 25:83 (2013b)

Mialdun, A., Legros, J.-C., Yasnou, V., Sechenyh V., Shevtsova, V.: Contribution to the benchmark for ternary mixtures: Measurement de Soret, diffusion and thermodiffusion coefficients in the ternary mixture THN/IBB/nC_{12} with 0.8/0.1/0.1 mass fractions in ground and orbital laboratories. Eur. Phys. J. E 38: 27 (2015).

NASA PIMS Handbook (2013). URL: https://pims.grc.nasa.gov/handbook/index.php. Accessed 18 January 2018

Ollé, J., Dubert, D., Gavaldà, J., Laverón-Simavilla, A., Ruiz, X., Shevtsova, V.: Onsite vibrational characterization of DCMIX2/3 experiments, Acta Astronaut. 140, 409-419 (2017)

PIMS website, http://pims.grc.nasa.gov/html/ISSAccelerationArchive.html, (2018). Accessed 18 January 2018

Rogers, M.J.B., Hrovat, K., Kelly, E., Reckart, T.: Accelerometer Data Analysis and Presentation Techniques. NASA Lewis Research Center. Clevehand, Ohio (1997)

Sáez, N., Ruiz, X., Gavaldà, Jna., Shevtsova, V.: Comparative Analyses of ESA, NASA and JAXA signals of acceleration during the SODI-IVIDIL experiment. Microgravity Sci. Tec. 26, 57-64 (2014)

Santos, C.I.A.V., Shevtsova, V., Burrows, H.D., Ribeiro, A.C.F.: Optimization of Taylor dispersion technique for measurement of mutual diffusion in benchmark mixtures. Microgravity Sci. Technol. 28: 459 (2016)

Seo, S.: A Review and Comparison of Methods for Detecting Outliers in Univariate Data Sets. Master Thesis, University of Pittsburgh. (2006)

Shannon, C. E.: A mathematical theory of communication. Bell System Tech. J. 27, 379-423 (1948)

Shevtsova, V., Santos, C., Sechenyh, V., Legros, J.C., Mialdun, A.: Diffusion and Soret in ternary mixtures. Preparation of the DCMIX2 experiment on the ISS. Microgravity Sci. Tec. 25, 275–283 (2014)

Yan, Y., Shevtsova, V., Saghir, M.Z.: Numerical study of low frequency g-jitter effect on thermal diffusion. FDMP J. 1 (4), 315–328 (2005)

Figure captions

Fig. 1. Minute by minute evolution of RMS and SEN in the three spatial directions, associated to DCMIX2 experiment, Run7.

Fig. 2. SEN values calculated for S1 (a) and S2 (b) sensors, in the three spatial directions, during DCMIX2 experiment, Run 16. Black rectangle indicates the EVA period.

Fig. 3. SEN values calculated for S1 (a), S2 (b), S3 (c) and S4 (d) sensors, in the three spatial directions, during DCMIX2 experiment, Run 1b.

Fig. 4. SEN values calculated for S1 (a), S2 (b), S3 (c) and S4 (d) sensors, in the three spatial directions, during DCMIX3 experiment, Run 20a. Black rectangle indicated the docking period.

Fig. 5. SEN values calculated for S1 (a), S2 (b), S3 (c) and S4 (d) sensors, in the three spatial directions, during DCMIX3 experiment, Run 6.

Fig. 6. RMS warning map of S1 (a) and S2 (b) sensors, DCMIX2, Run 16 with EVA event (black rectangle). Marks indicating when the RMS exceeds the ISS vibratory limit requirements.

Fig. 7. RMS warning map of S1 (a), S2 (b), S3 (c) and S4 (d) sensors, DCMIX2, Run 1b. Marks indicating when the RMS exceeds the ISS vibratory limit requirements.

Fig. 8. RMS warning map of S1 (a), S2 (b), S3 (c) and S4 (d) sensors, DCMIX3, Run 20a with docking event (black rectangle). Marks indicating when the RMS exceeds the ISS vibratory limit requirements.

Fig. 9. RMS warning map of S1 (a), S2 (b), S3 (c) and S4 (d) sensors, DCMIX3, Run 6. Marks indicating when the RMS exceeds the ISS vibratory limit requirements.

Fig. 10. Scatterplot and Spearman's Coefficient of**:** a) DCMIX2, Run 16, S1-S2, a_z**-**a_z components, b) DCMIX3, Run 20a, S1-S2, a_z-a_z components.

Fig. 11. Coherence function in all three direction, calculated for**:** Run 16, DCMIX2: a) S1-S2, Run 20a, DCMIX3, b) S1-S2, c) S1-S3 and d) S1-S4.

Fig. 12. Detailed magnification for low frequency interval of Fig. 11.

Table 1: Selected episodes during DCMIX2/3 experiments.

Experiments	Date	Spacecraft type	Port	Disturbance		Sensors used
				Kind	Main direction	
DCMIX2	Run 1b 10/12/2013	-	-	Quiescent period		Es03 (S1) SAMS2 121f03 (S2) SAMS2 121f08 (S3) SAMS2 121f05 (S4)
	Run 16 26/12/2013	-	-	EVA	All directions	Es03 (S1) SAMS2 121f03 (S2)
DCMIX3	Run 6 27/09/2016	-	-	Quiescent period		Es03 (S1) SAMS2 121f03 (S2) SAMS2 121f08 (S3) SAMS2 121f05 (S4)
	Run 20a 21/10/2016	Soyuz MS-02/48s	Zenith port (Poisk module)	Docking	$+Z_A$	Es03 (S1) SAMS2 121f03 (S2) SAMS2 121f08 (S3) SAMS2 121f05 (S4)

Table 2: Sensors used and their characteristics.

Experiments		DCMIX2			DCMIX3		
Sensors	Module	Localization	Sampling rate (Hz)	Cutoff (Hz)	Localization	Sampling rate (Hz)	Cutoff (Hz)
S1	Glovebox	LAB1S2 MSG Ceiling Plate Y1-B1 Y2-A1	250	101.4	LAB1S2 MSG Floor Plate OASIS	250	101.4
S2	Destiny	LAB1O1 ER2 Lower Z Panel	500	200	LAB1O1 ER2 Lower Z Panel	500	200
S3	Columbus	COL1A1 ER3 Seat Track near D1	1000	400	COL1A3 EPM near PK-4	500	200
S4	Kibo	JPM1F5 ER4 Drawer 2	500	200	JPM1F5 ER4 Drawer 2	500	200

NOTE: LAB1S2 - United States laboratory in MSG - Microgravity Glovebox; LAB1O1 - United States laboratory; COL1A1 - Columbus laboratory (https://pims.grc.nasa.gov/); JPM1F5 - Japanese Experiment Module (https://www1.grc.nasa.gov/space/iss-research/acceleration)

Table 3: Descriptive statistics and Gaussian characteristics of the signals

Experiments	Period/ disturbance	Sensors	Unimodal/ Bimodal			Skewness			Excess of kurtosis			Outliers (%)		
			x_A	y_A	z_A	x_A	y_A	z_A	x_A	y_A	z_A	x_A	y_A	z_A
DCMIX2	EVA (Run 16)	S1	2	2	1	-	-	0.032	-	-	21.62	4.2	1.8	8.5
		S2	2	1	1	-	0.009	0.134	-	- 0.24	- 0.23	5.8	8.5	9.3
	Quiescent (Run 1b)	S1	2	2	2	-	-	-	-	-	-	2.9	3.8	5.7
		S2	1	1	1	-0.003	-0.087	0.144	-0.09	0.04	-0.15	9.0	9.1	9.5
		S3	2	2	1	-	-	-0.043	-	-	-0.40	0.0	5.4	9.3
		S4	1	1	1	0.026	-0.031	-0.137	-0.10	-0.51	-0.04	8.6	6.7	8.6
DCMIX3	Docking (Run 20a)	S1	1	2	1	-0.001	-	0.002	-0.66	-	-0.14	6.4	5.8	6.2
		S2	2	2	1	-	-	-0.001	-	-	-0.30	0.0	2.0	8.6
		S3	1	1	1	-0.012	-0.522	-0.005	28.27	201.28	13.66	10.5	10.4	10.2
		S4	1	1	1	-0.002	-0.001	0.006	-0.50	-0.30	0.05	8.0	8.5	9.1
	Quiescent (Run 6)	S1	2	1	1	-	0.000	0.000	-	-0.64	-0.51	5.9	6.1	7.2
		S2	2	2	1	-	-	-0.047	-	-	-0.30	0.1	4.2	8.4
		S3	1	1	1	0.005	-0.001	0.008	0.16	0.09	1.07	9.3	8.8	9.9
		S4	1	1	1	-0.002	-0.008	-0.004	-0.43	-0.35	0.02	8.4	8.5	9.2

1: Unimodal, 2: Bimodal

Table 4: FFI for both experiments and considered runs.

Experiments	**Run**	**Period/ disturbance**	**Sensors**	**FFI_x, FFI_y, FFI_z < 20Hz**	**FFI_x, FFI_y, FFI_z < 1Hz**	**Frequency (Hz)**	**Intensity of maximum frequency x 10^{-4}(g^2/Hz)**
DCMIX2	16	EVA	S1	3.2, 2.5, 2.5 (2.7)	4.4, 4.6, 4.4 (4.5)	73.1, 73.1, 73.1	2.51 , 1.85, 2.1
			S2	4.4, 4.9, 4.9 (4.8)	5.3, 5.4, 5.1 (5.3)	98.3, 98.3, 60	101.5, 7.28, 16
	1b	Quiescent	S1	3.1, 3.0, 2.9 (3.0)	4.7, 4.9, 4.8 (4.8)	73.1, 73.1, 73.1	4.4, 1.0, 0.47
			S2	3.6, 3.9, 4.4 (4.0)	4.9, 4.9, 4.7 (4.8)	95.44, 60, 60	12.32, 1.95, 7.8
			S3	3.6, 3.6, 3.8 (3.7)	4.5, 4.9, 4.9 (4.8)	15, 94.72, 94.72	0.0006,0.002, 0.0003
			S4	0.9, 3.0, 2.5 (2.1)	3.4, 3.5, 3.5 (3.4)	15, 58.18, 58.18	0.14, 0.01, 0.02
DCMIX3	20a	Docking	S1	2.6,2.8,2.6 (2.7)	4.6,4.5, 4.4 (4.5)	73.1, 73.1, 73.1	1.9, 1.1, 1.0
			S2	5.8, 6.2, 5.9 (6)	6.4,6.6, 6.3 (6.4)	98.26, 98.26, 98.26	1454, 210, 34
			S3	0.94, 1.1,1 (1)	1.7,2.0,1.7 (1.8)	66.47, 66.47, 66.47	0.01, 0.018,0.0016
			S4	2.7,3.5,3.2 (3.2)	3.9, 4, 3.9 (3.9)	66.47, 66.47, 66.47	0.09, 0.8,0.66
	6	Quiescent	S1	2.7,3.3,3 (3)	5.2,4.9,4.7 (4.9)	73.1, 73.1, 73.1	3.1, 1.1, 1.2
			S2	6,6.4,6.1 (6.2)	6.5,7,6.3 (6.6)	98.26, 98.26, 98.26	2018, 281, 68
			S3	0.5,.9,1.3 (0.9)	2.2,2.3,1.9 (2.1)	66.47, 66.47, 66.47	0.015, 0.02, 0.0009
			S4	3.1,3.3,3.6 (3.3)	4.3, 4.3, 4.1 (4.2)	66.47, 66.47, 90.3	0.09, 0.37, 0.7

Table 5: Spectral fingerprints of several sources of mechanical disturbances.

Frequency band	Sensor (type and position)	Disturbance source	Spectral fingerprint (Hz)
(*) 0.01 < f < 8 Hz	MAMS HiRAP006 at LAB1O2, ER1, Lockers 3,4 SAMS2 121f08006 at COL1A1, ER3, Seat Track near D1 SAMS2 121f05006 at JPM1F5, ER4, Drawer 2	Progress Docking	0.01 - 0.8 0.7 (after the event) 0.01 - 1.5
	MAMS HiRAP006 at LAB1O2, ER1, Lockers 3,4 SAMS2 121f08006 at COL1A2, ER3, Seat Track near D1 SAMS2 121f03006 at LAB1O1, ER2, Lower Z Panel SAMS2 121f05 at JPM1F5, ER4, Drawer 2	Progress Undocking	0.2, 0.6, 1.8 0.7 (after the event) 1.3, 2, 3, 3,3, 3.7 (during the previous Russian attitude control period) 0.01 - 3
	MAMS HiRAP006 at LAB1O2, ER1, Lockers 3,4121f03	Progress Reboost	0.01 - 1
	MAMS HiRAP006 at LAB1O2, ER1, Lockers 3,4	Progress Propellant Line Purgue	0.5 – 2
	SAMS2 121f02 at LAB1O2, ER1, Drawer 1 SAMS2 121f05006 at JPM1F5, ER4, Drawer 2	Automated Transfer Vehicles, ATV, docking	< 6 0.01 - 0.3, 0.6
	SAMS2 121f08 at COL1A1, ER3, Seat Track near D1 SAMS2 121f05 at JPM1F5, ER4, Drawer 2	Automated Transfer Vehicle, ATV, reboost	0.01 – 2 0.01 – 2
	MAMS HiRAP at LAB1O2, ER 1, Lockers 3,4 SAMS2 121f03 at LAB1O1, ER2, Lower Z Panel	Soyuz Docking	< 6
	SAMS2 121f02 at LAB1O2, ER1, Drawer 1 SAMS2 121f03 at LAB1O1, ER2, Lower Z Panel	Soyuz Undocking	
	SAMS2 121f05 at JPM1F5, ER4, Drawer 2	Solar Array Efficiency Test, **SAET** (Russian Segment thrusters were used for attitude maintenance during test, while US Control Moment Gyros, CMGs, were used before and after it)	0.5 - 1.5
	SAMS2 121f05 at LAB1O1, ER2, Upper Z Panel	Cycle Ergometer with Vibration Isolation System, **CEVIS**	0.1 – 3
	SAMS2 121f03006 at LAB1O1, ER2, Lower Z Panel	**Crew** exercise	< 3
	SAMS2 121f03 at LAB1O1, ER2, Lower Z Panel	Velosiped, **VELO-VB-3M**	2.3, 4.6
	SAMS2 121f03 at LAB1O1, ER2, Lower Z Panel SAMS2 121f05006 at JPM1F5, ER4, Drawer 2	Optimized Propellant Maneuver, **OPM**	0.01 - 6
	MAMS HiRAP at LAB1O2, ER1, Lockers 3,4	**Crew** Glovebox Push-Off *(important for Glovebox data interpretation !!!)*	near 7.5
(*) This band includes the frequency range of the structural modes of the Station. These modes could be excited when short impulsive forces –reboostings- mechanically excite large components of the structure as, for instance, the main Truss and/or the solar panels. Also when different Station maneuvers are effected in order to prepare spacecraft dockings or undockings (for instance, in case of docking, a typical ISS maneuver could start from -XVV/+ZLV TEA attitude to –XVV/+ZLV and back again to -XVV/+ZLV TEA; similarly, an ISS maneuver for undocking could start from +XVV/+ZLV TEA attitude to +ZVV/-XLV and then back again to +XVV/+ZLV TEA).			
(**) 8 < f < 200 Hz	SAMS2 121f02 at LAB1O2, ER1, Drawer 1	Ku-Band Antennas	5 – 20
	SAMS2 121f02 at LAB1O2, ER1, Drawer 1	Russian **SKV** Air Conditioner	23.5
	SAMS2 121f03 at LAB1O1, ER2, Lower Z Panel SAMS2 121f05 at JPM1F5, ER4, Drawer 2	JEM Airlock Vacuum Pump activity	24 (2nd through 4th harmonics) 24 (2nd through 4th harmonics)
	SAMS2 121f02 at LAB1O2, ER1, Drawer 1	Resistive Exercise Device, **RED**	< 30
	MAMS HiRAP at LAB1O2, ER1, Lockers 3,4	Urine Processing Assembly, **UPA**	3.6, 33.3
	SAMS2 121f03 at LAB1O1, ER2, Lower Z Panel	**Robo**naut operations	47.4
	SAMS2 121f04 at LAB1O2, ER1, Lower Z Panel	Internal Thermal Control System, **ITCS**	35 - 60 (also 130, 195)
	SAMS TSH-ES03 at LAB1S2, MSG, Ceiling Plate Y1-B1 Y2-A1	Microgravity Science Glovebox Operations, **MSG**	46 - 47 (normal fans mode) 73 (open fans mode)
	SAMS2 121f02 at LAB1O2, ER1, Drawer 1	Gas Analysis System for Metabolic Analysis of Physiology, **GASMAP**	57 - 58 (fan) 54 - 62 (pumps)
	SAMS2 121f02 at LAB1O2, ER1, Drawer 1	Medical Equipment Computer, **MEC**	59.5 – 70.4
	SAMS2 121f02 at LAB1O2, ER1, Drawer 1	Periodic Fitness Evaluation, **PFE**	68 – 72
	SAMS2 121f05 at JPM1F5, ER4, Drawer 2	**FROST** Stirling Cooler	80
	SAMS2 121f08 at COL1A3, EPM, near PK-4	Centrifuge Rotor of **Biolab**	86.5, 107.3
	SAMS2 121f03 at LABO1, ER2, Lower Z Panel	Station Control Moment Gyroscopes, **CMGs**	110
	SAMS2 121f02 at LAB1S2, MSG, Upper Left Seat Track	General Laboratory Active Cryogenic ISS Experimental Refrigerator, **GLACIER**	60, 120, 180 (Start-up)
	SAMS2 121f08 at COL1A2, ER3, Seat Track near D1	Columbus General Laboratory Active Cryogenic ISS Experimental Refrigerator, **GLACIER-3**	116 - 120 (start-up) near 80 (steady state)
	SAMS2 121f03 at LAB1O1, ER2, Lower Z Panel	Common Cabin Air Assembly, **CCAA**	53 - 128 (inlet variable speed fan) 95 - 100 (water separator fan)
	SAMS2 121f08 at COL1A3, EPM, near PK-4	Electro-Magnetic Levitator, **EML**, in the European Drawer Rack	50 – 90 140 - 170
	SAMS TSH-ES06 at LAB1S4, Fluid Integrated Rack(FIR)	**LAB** Aft Port IMV fan	141.7
	SAMS2 121f04 at LAB1O2, ER1, Lower Z Panel	InterModule Ventilation fans, **IMV**	139 – 145
(**) This band includes the frequency range of the Station internal subsystems, like pumps and fans, used in the different kind of scientific experiments as well as in life support equipment.			

Fig1

Click here to download line figure Fig01.tif

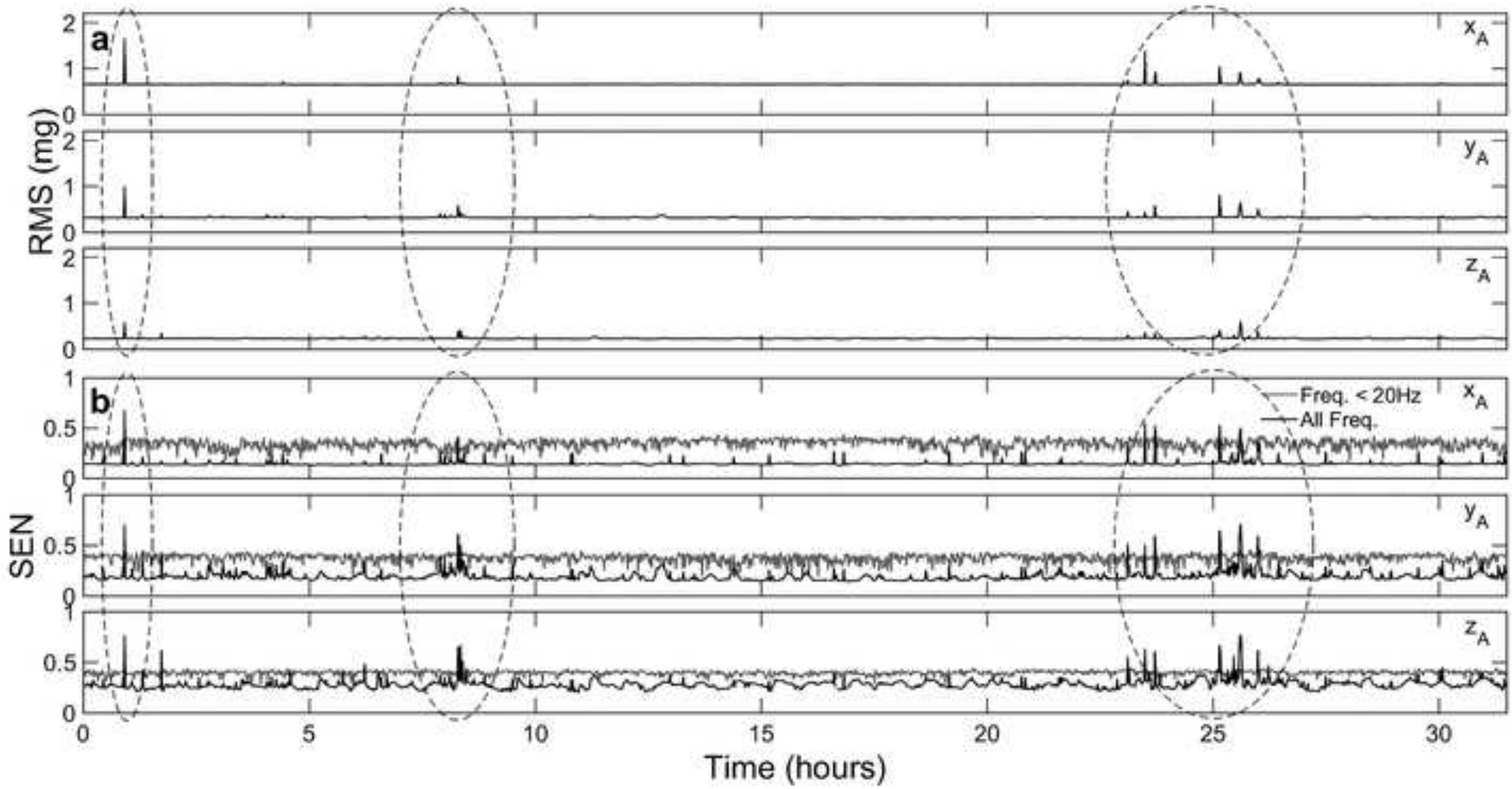

Fig2

Click here to download line figure Fig02.tif

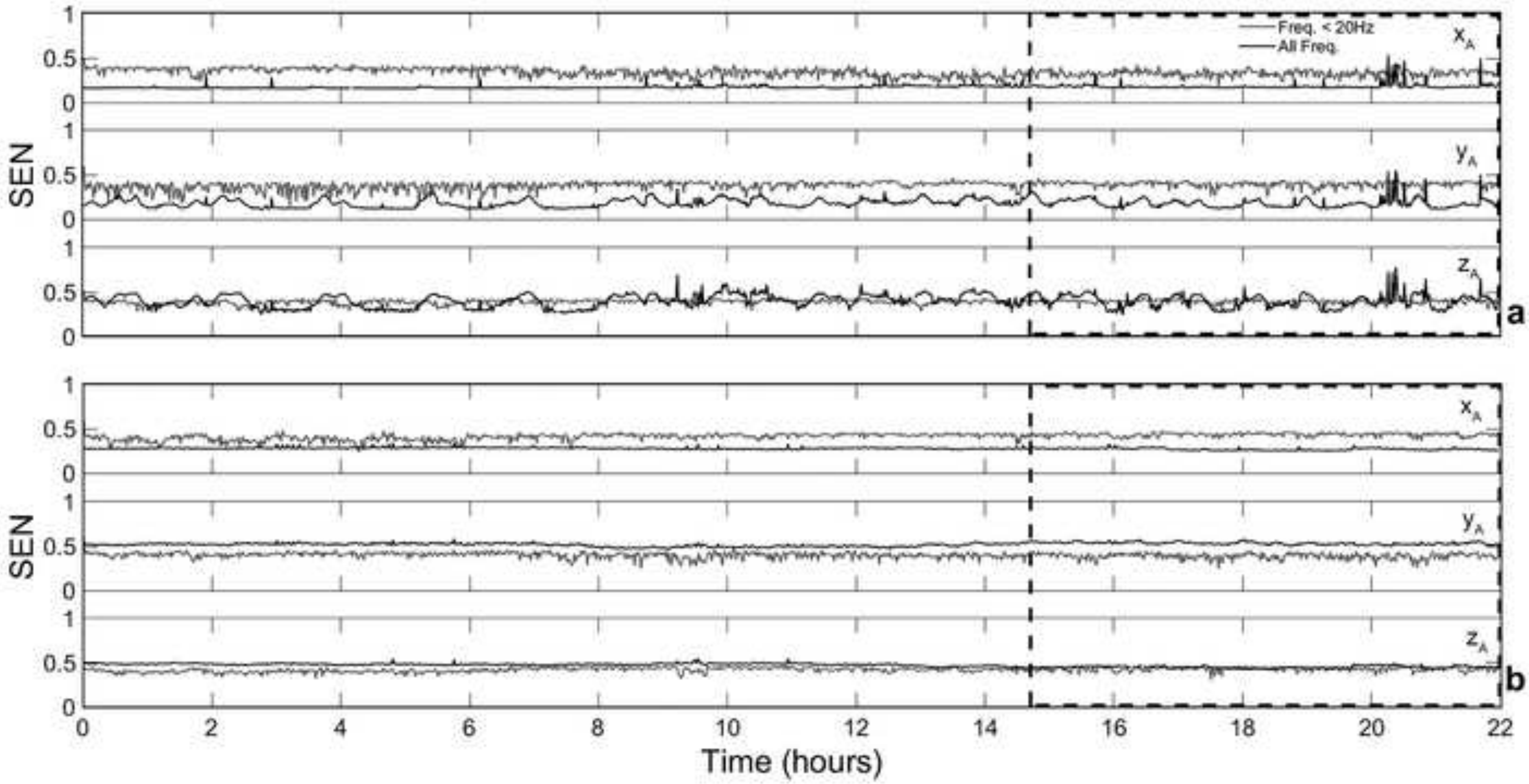

Fig3

Click here to download line figure Fig03.tif

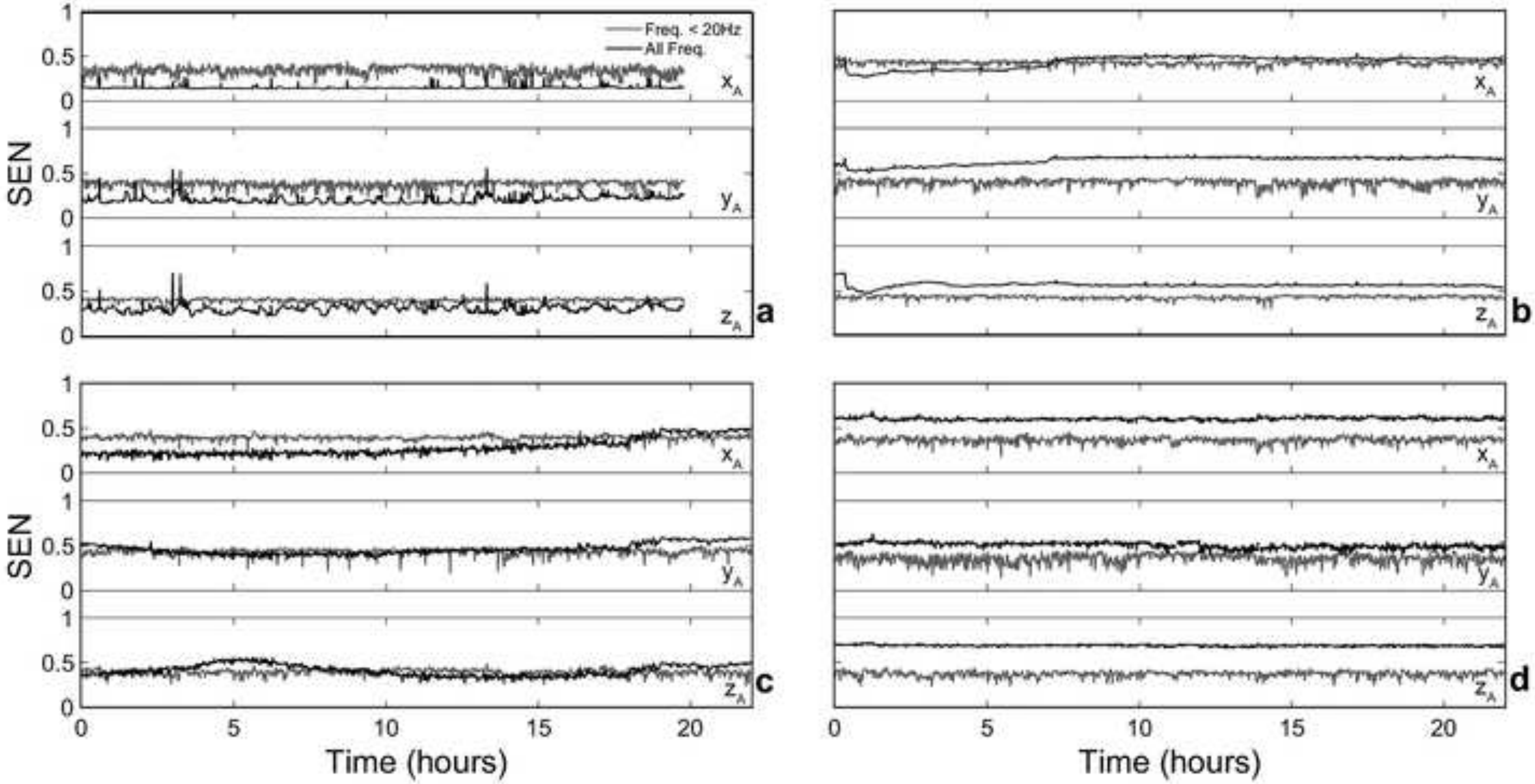

Fig4

Click here to download line figure Fig04.tif

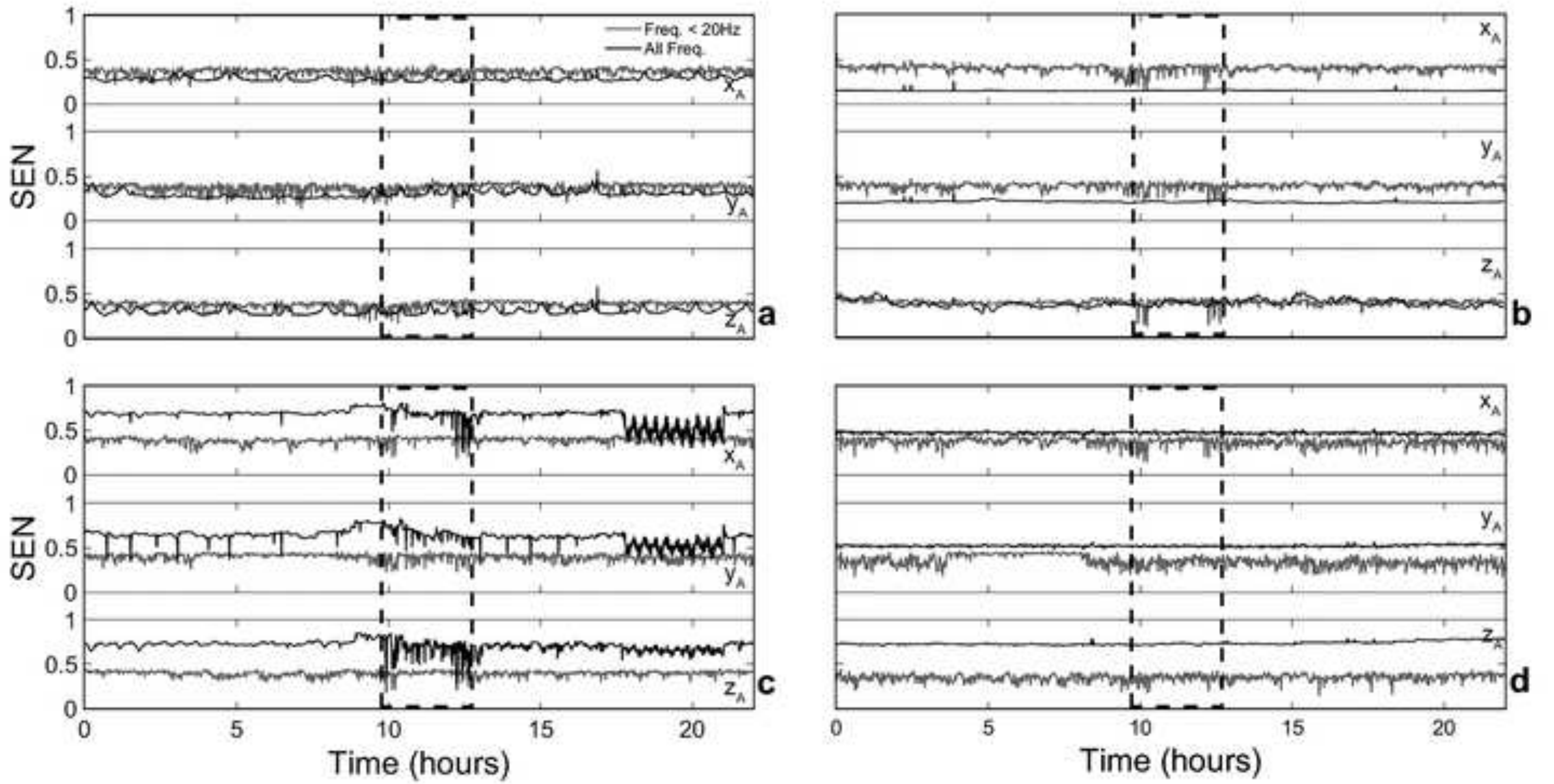

Fig5

Click here to download line figure Fig05.tif

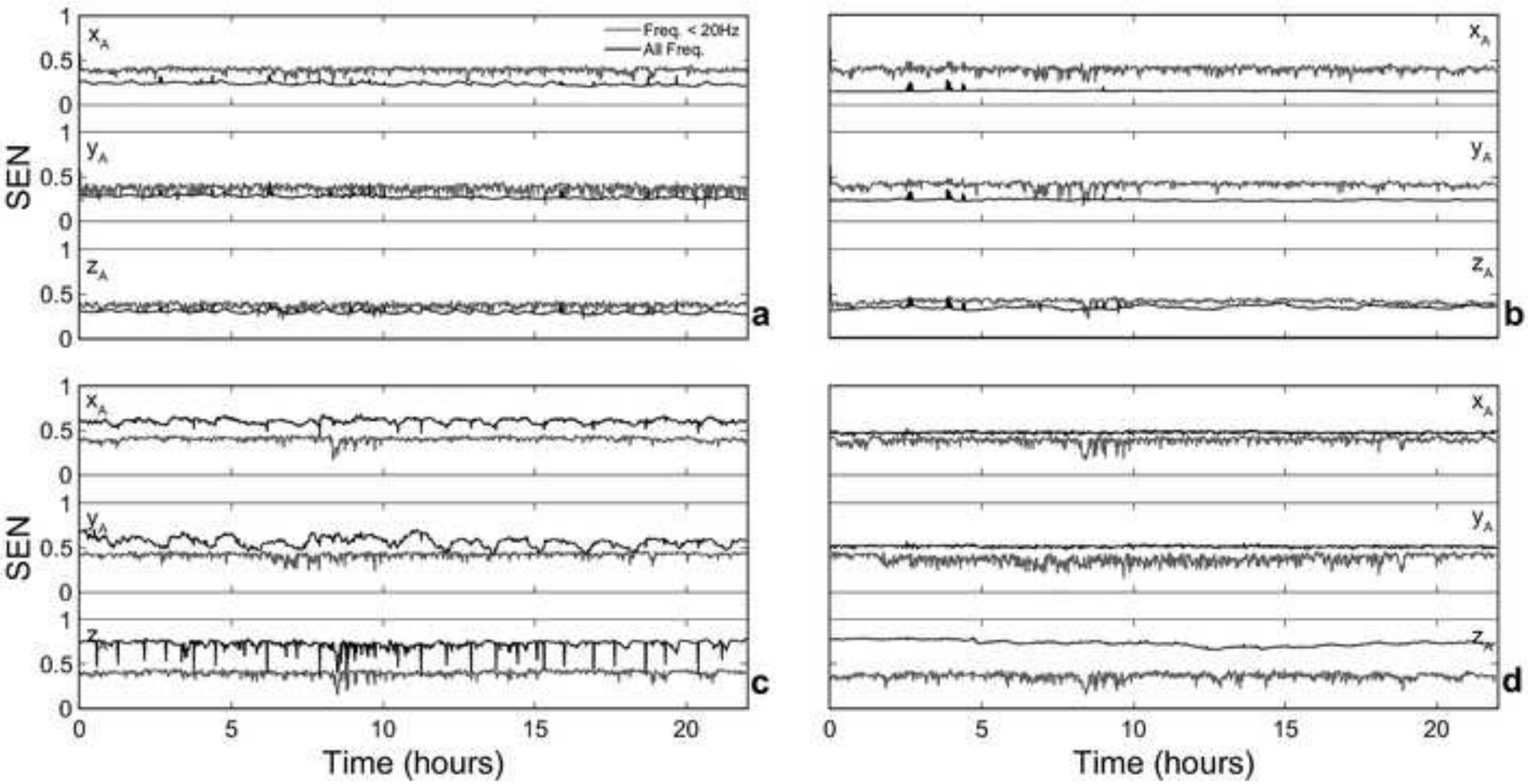

Fig6

Click here to download colour figure Fig06.tif

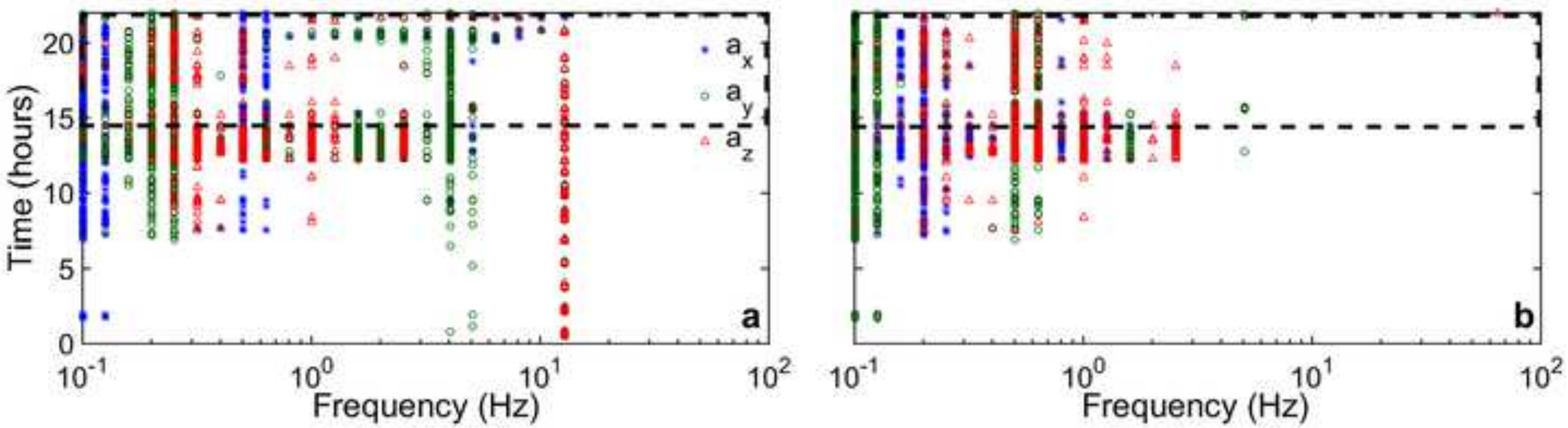

Fig7

Click here to download colour figure Fig07.tif

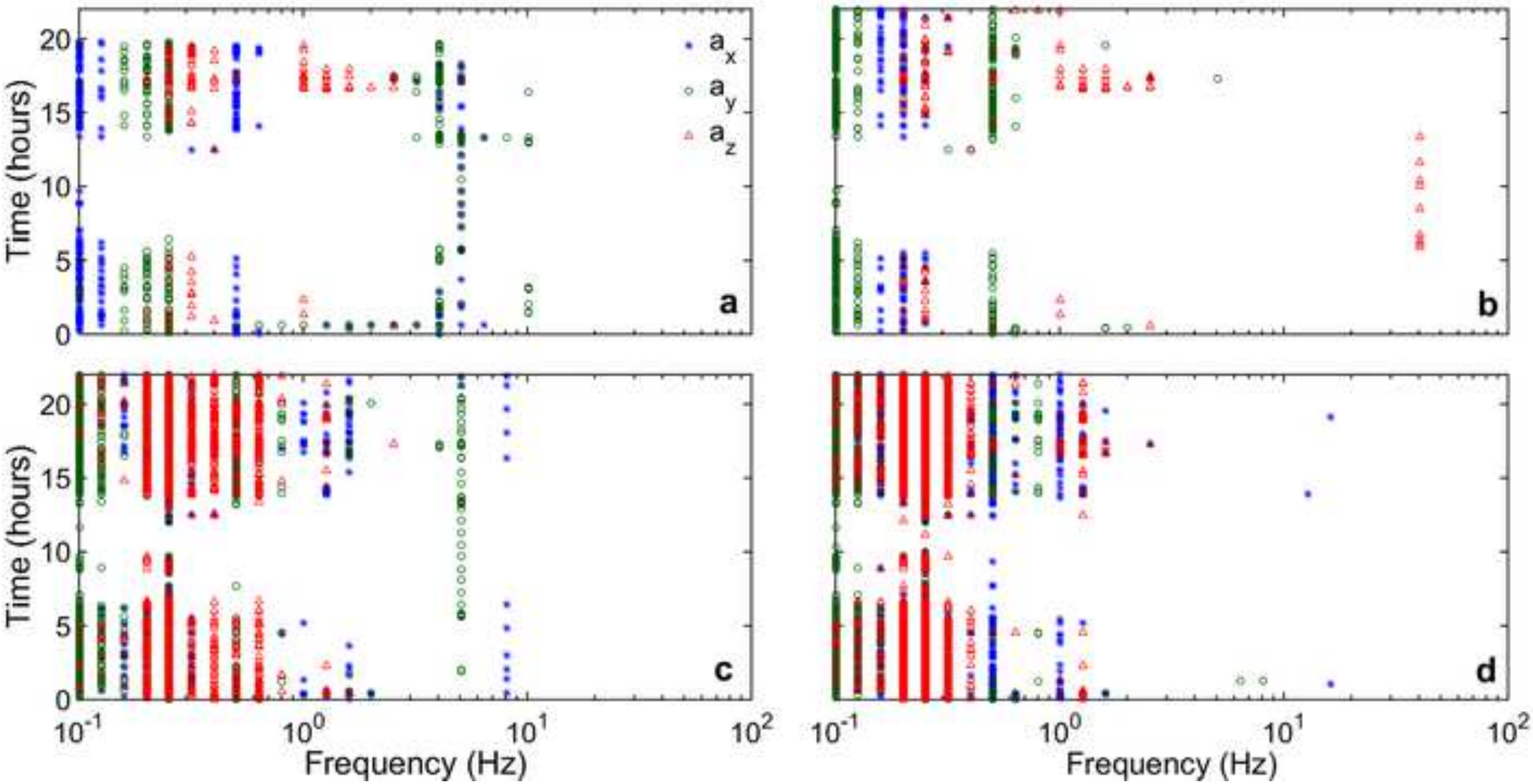

Fig8

Click here to download colour figure Fig08.tif

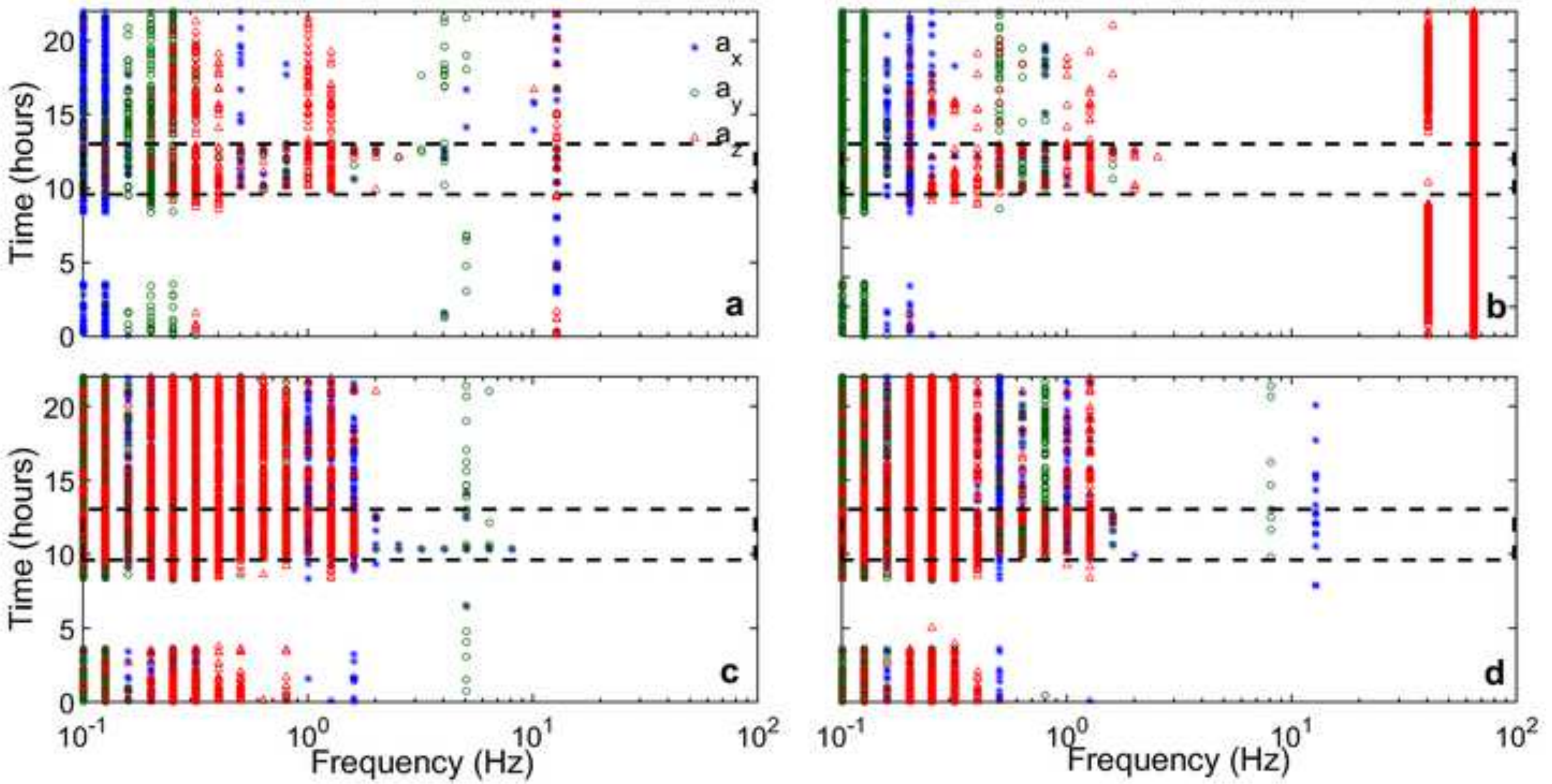

Fig9

Click here to download colour figure Fig09.tif

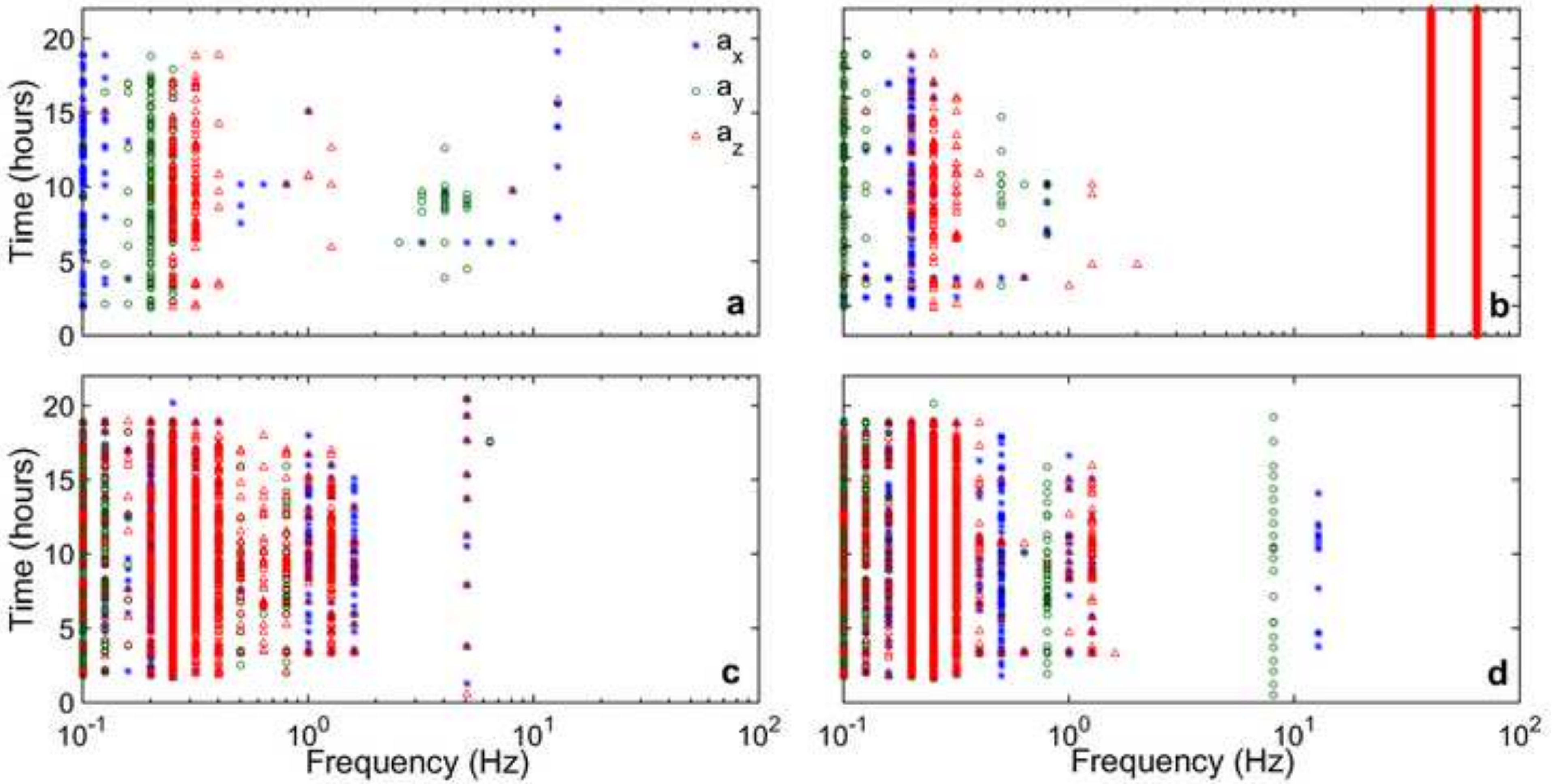

Fig10

Click here to download line figure Fig10.tif

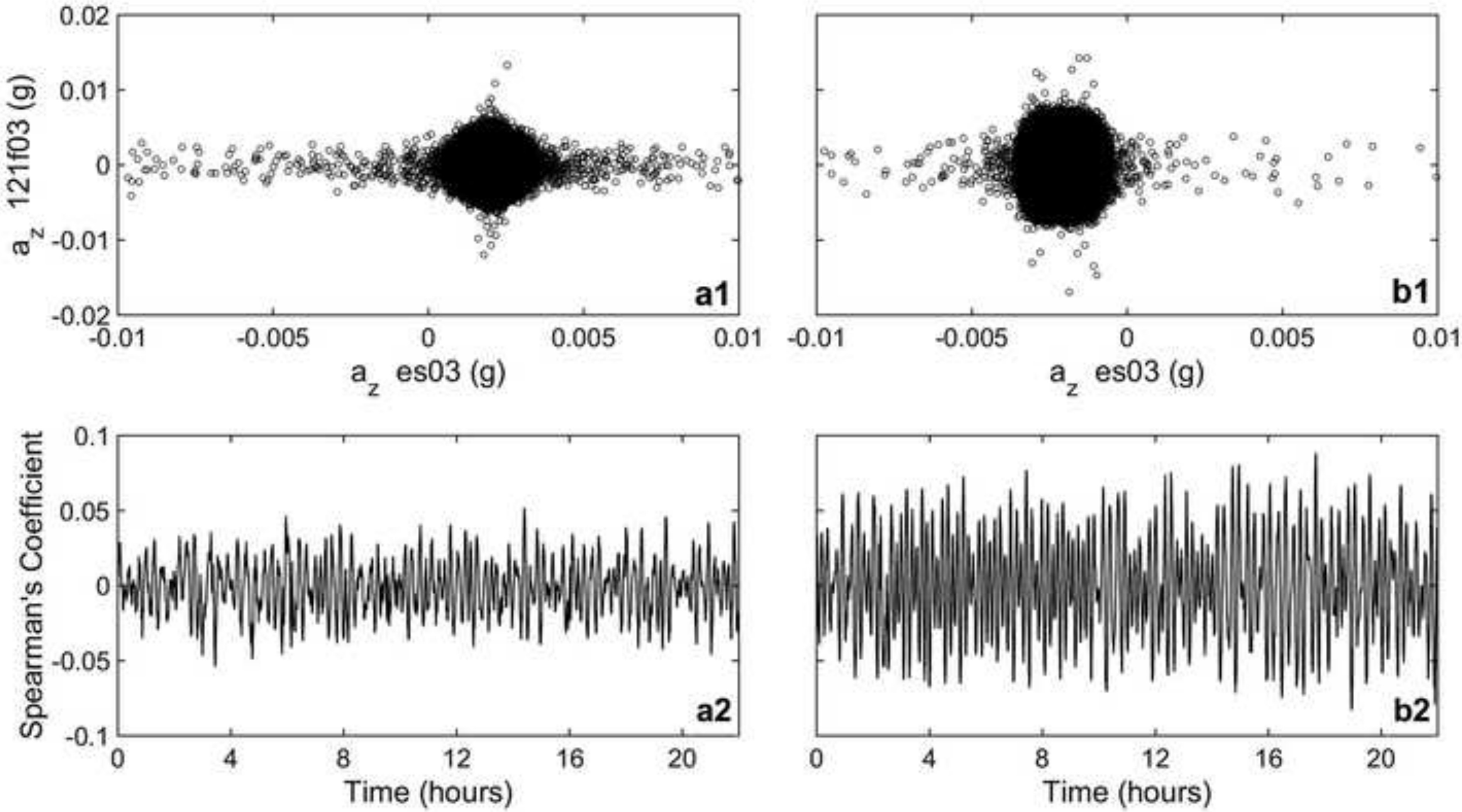

Fig11

Click here to download line figure Fig11.tif

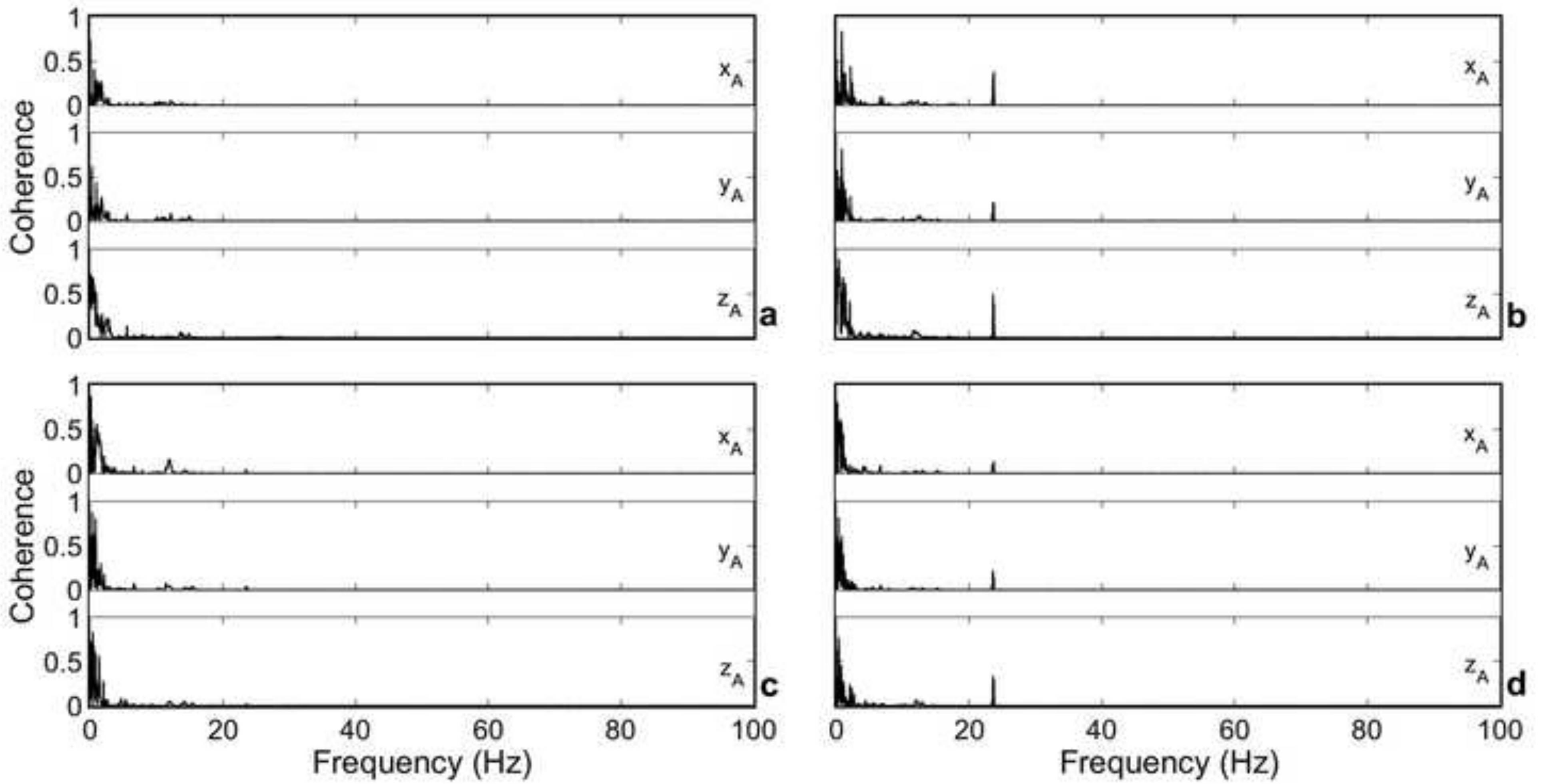

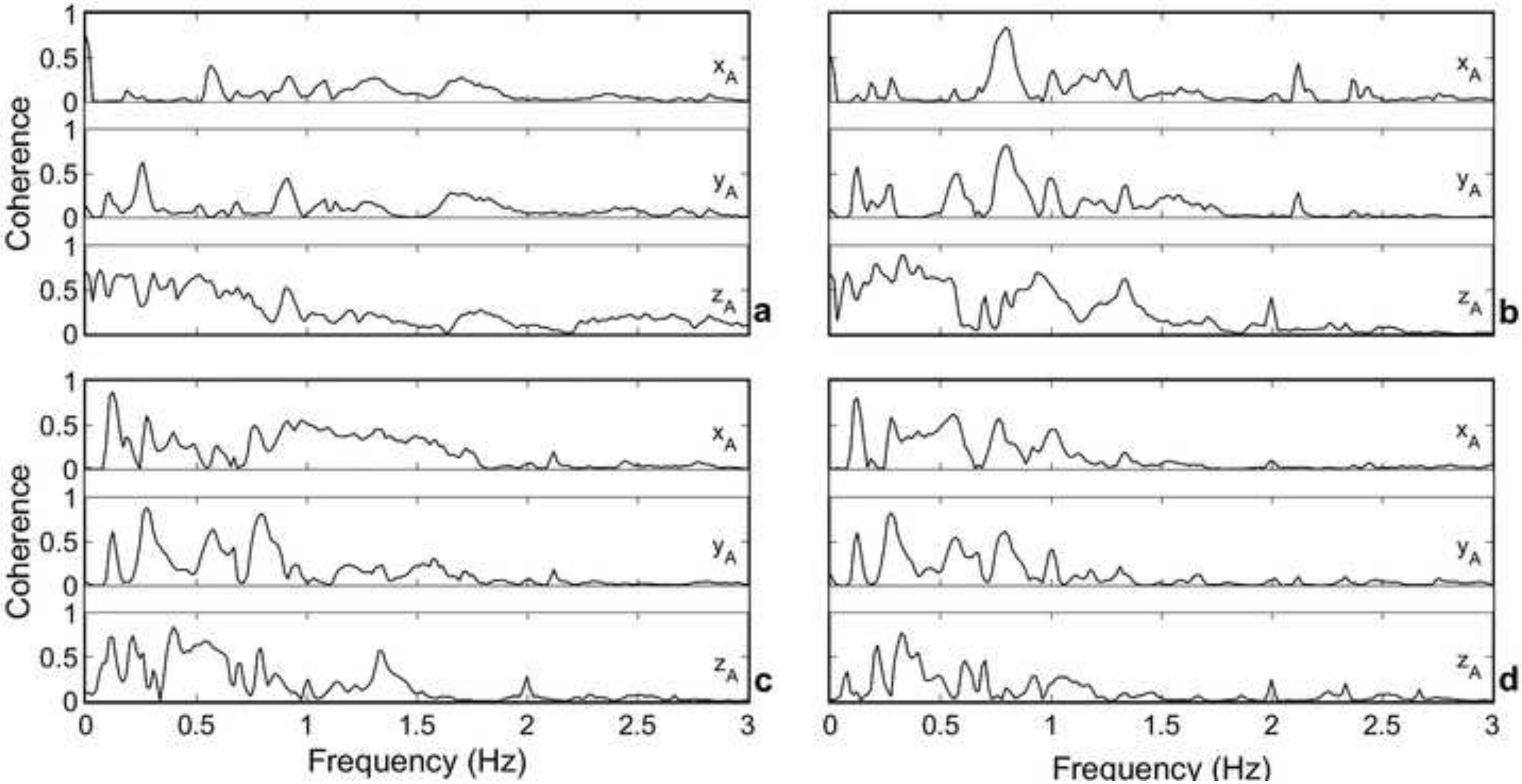
Coherence
1
0.5
0
x_A
y_A
z_A
a
b
c
d
0
0.5
1
1.5
2
2.5
3
Frequency (Hz)

table1 Click here to download table Table 1.docx

Table 1: Selected episodes during DCMIX2/3 experiments.

Experiments	Date	Spacecraft type	Port	Disturbance		Sensors used
				Kind	Main direction	
DCMIX2	Run 1b 10/12/2013	-	-	Quiescent period		Es03 (S1) SAMS2 121f03 (S2) SAMS2 121f08 (S3) SAMS2 121f05 (S4)
	Run 16 26/12/2013	-	-	EVA	All directions	Es03 (S1) SAMS2 121f03 (S2)
DCMIX3	Run 6 27/09/2016	-	-	Quiescent period		Es03 (S1) SAMS2 121f03 (S2) SAMS2 121f08 (S3) SAMS2 121f05 (S4)
	Run 20a 21/10/2016	Soyuz MS-02/48s	Zenith port (Poisk module)	Docking	$+Z_A$	Es03 (S1) SAMS2 121f03 (S2) SAMS2 121f08 (S3) SAMS2 121f05 (S4)

Table 2: Sensors used and their characteristics.

Experiments		DCMIX2			DCMIX3		
Sensors	**Module**	**Localization**	**Sampling rate (Hz)**	**Cutoff (Hz)**	**Localization**	**Sampling rate (Hz)**	**Cutoff (Hz)**
S1	Glovebox	LAB1S2 MSG Ceiling Plate Y1-B1 Y2-A1	250	101.4	LAB1S2 MSG Floor Plate OASIS	250	101.4
S2	Destiny	LAB1O1 ER2 Lower Z Panel	500	200	LAB1O1 ER2 Lower Z Panel	500	200
S3	Columbus	COL1A1 ER3 Seat Track near D1	1000	400	COL1A3 EPM near PK-4	500	200
S4	Kibo	JPM1F5 ER4 Drawer 2	500	200	JPM1F5 ER4 Drawer 2	500	200

NOTE: LAB1S2 - United States laboratory in MSG - Microgravity Glovebox; LAB1O1 - United States laboratory; COL1A1 - Columbus laboratory (https://pims.grc.nasa.gov/); JPM1F5 - Japanese Experiment Module (https://www1.grc.nasa.gov/space/iss-research/acceleration)

Table 3: Descriptive statistics and Gaussian characteristics of the signals

Experiments	Period/ disturbance	Sensors	Unimodal/ Bimodal			Skewness			Excess of kurtosis			Outliers (%)		
			x_A	y_A	z_A	x_A	y_A	z_A	x_A	y_A	z_A	x_A	y_A	z_A
DCMIX2	EVA (Run 16)	S1	2	2	1	-	-	0.032	-	-	21.62	4.2	1.8	8.5
		S2	2	1	1	-	0.009	0.134	-	- 0.24	- 0.23	5.8	8.5	9.3
	Quiescent (Run 1b)	S1	2	2	2	-	-	-	-	-	-	2.9	3.8	5.7
		S2	1	1	1	-0.003	-0.087	0.144	-0.09	0.04	-0.15	9.0	9.1	9.5
		S3	2	2	1	-	-	-0.043	-	-	-0.40	0.0	5.4	9.3
		S4	1	1	1	0.026	-0.031	-0.137	-0.10	-0.51	-0.04	8.6	6.7	8.6
DCMIX3	Docking (Run 20a)	S1	1	2	1	-0.001	-	0.002	-0.66	-	-0.14	6.4	5.8	6.2
		S2	2	2	1	-	-	-0.001	-	-	-0.30	0.0	2.0	8.6
		S3	1	1	1	-0.012	-0.522	-0.005	28.27	201.28	13.66	10.5	10.4	10.2
		S4	1	1	1	-0.002	-0.001	0.006	-0.50	-0.30	0.05	8.0	8.5	9.1
	Quiescent (Run 6)	S1	2	1	1	-	0.000	0.000	-	-0.64	-0.51	5.9	6.1	7.2
		S2	2	2	1	-	-	-0.047	-	-	-0.30	0.1	4.2	8.4
		S3	1	1	1	0.005	-0.001	0.008	0.16	0.09	1.07	9.3	8.8	9.9
		S4	1	1	1	-0.002	-0.008	-0.004	-0.43	-0.35	0.02	8.4	8.5	9.2

1: Unimodal, 2: Bimodal

Table 4: FFI for both experiments and considered runs.

Experiments	Run	Period/ disturbance	Sensors	FFI_x, FFI_y, FFI_z < 20Hz	FFI_x, FFI_y, FFI_z < 1Hz	Frequency (Hz)	Intensity of maximum frequency x 10^{-4}(g^2/Hz)
DCMIX2	16	EVA	S1	3.2, 2.5, 2.5 (2.7)	4.4, 4.6, 4.4 (4.5)	73.1, 73.1, 73.1	2.51 , 1.85, 2.1
			S2	4.4, 4.9, 4.9 (4.8)	5.3, 5.4, 5.1 (5.3)	98.3, 98.3, 60	101.5, 7.28, 16
	1b	Quiescent	S1	3.1, 3.0, 2.9 (3.0)	4.7, 4.9, 4.8 (4.8)	73.1, 73.1, 73.1	4.4, 1.0, 0.47
			S2	3.6, 3.9, 4.4 (4.0)	4.9, 4.9, 4.7 (4.8)	95.44, 60, 60	12.32, 1.95, 7.8
			S3	3.6, 3.6, 3.8 (3.7)	4.5, 4.9, 4.9 (4.8)	15, 94.72, 94.72	0.0006,0.002, 0.0003
			S4	0.9, 3.0, 2.5 (2.1)	3.4, 3.5, 3.5 (3.4)	15, 58.18, 58.18	0.14, 0.01, 0.02
DCMIX3	20a	Docking	S1	2.6,2.8,2.6 (2.7)	4.6,4.5, 4.4 (4.5)	73.1, 73.1, 73.1	1.9, 1.1, 1.0
			S2	5.8, 6.2, 5.9 (6)	6.4,6.6, 6.3 (6.4)	98.26, 98.26, 98.26	1454, 210, 34
			S3	0.94, 1.1,1 (1)	1.7,2.0,1.7 (1.8)	66.47, 66.47, 66.47	0.01, 0.018,0.0016
			S4	2.7,3.5,3.2 (3.2)	3.9, 4, 3.9 (3.9)	66.47, 66.47, 66.47	0.09, 0.8,0.66
	6	Quiescent	S1	2.7,3.3,3 (3)	5.2,4.9,4.7 (4.9)	73.1, 73.1, 73.1	3.1, 1.1, 1.2
			S2	6,6.4,6.1 (6.2)	6.5,7,6.3 (6.6)	98.26, 98.26, 98.26	2018, 281, 68
			S3	0.5,.9,1.3 (0.9)	2.2,2.3,1.9 (2.1)	66.47, 66.47, 66.47	0.015, 0.02, 0.0009
			S4	3.1,3.3,3.6 (3.3)	4.3, 4.3, 4.1 (4.2)	66.47, 66.47, 90.3	0.09, 0.37, 0.7

Table 5: Spectral fingerprints of several sources of mechanical disturbances.

Frequency band	Sensor (type and position)	Disturbance source	Spectral fingerprint (Hz)
(*) 0.01 < f < 8 Hz	MAMS HiRAP006 at LAB1O2, ER1, Lockers 3,4 SAMS2 121f08006 at COL1A1, ER3, Seat Track near D1 SAMS2 121f05006 at JPM1F5, ER4, Drawer 2	Progress Docking	0.01 - 0.8 0.7 (after the event) 0.01 - 1.5
	MAMS HiRAP006 at LAB1O2, ER1, Lockers 3,4 SAMS2 121f08006 at COL1A2, ER3, Seat Track near D1 SAMS2 121f03006 at LAB1O1, ER2, Lower Z Panel SAMS2 121f05 at JPM1F5, ER4, Drawer 2	Progress Undocking	0.2, 0.6, 1.8 0.7 (after the event) 1.3, 2, 3, 3,3, 3.7 (during the previous Russian attitude control period) 0.01 - 3
	MAMS HiRAP006 at LAB1O2, ER1, Lockers 3,4121f03	Progress Reboost	0.01 - 1
	MAMS HiRAP006 at LAB1O2, ER1, Lockers 3,4	Progress Propellant Line Purgue	0.5 – 2
	SAMS2 121f02 at LAB1O2, ER1, Drawer 1 SAMS2 121f05006 at JPM1F5, ER4, Drawer 2	Automated Transfer Vehicles, ATV, docking	< 6 0.01 - 0.3, 0.6
	SAMS2 121f08 at COL1A1, ER3, Seat Track near D1 SAMS2 121f05 at JPM1F5, ER4, Drawer 2	Automated Transfer Vehicle, ATV, reboost	0.01 – 2 0.01 – 2
	MAMS HiRAP at LAB1O2, ER 1, Lockers 3,4 SAMS2 121f03 at LAB1O1, ER2, Lower Z Panel	Soyuz Docking	< 6
	SAMS2 121f02 at LAB1O2, ER1, Drawer 1 SAMS2 121f03 at LAB1O1, ER2, Lower Z Panel	Soyuz Undocking	
	SAMS2 121f05 at JPM1F5, ER4, Drawer 2	Solar Array Efficiency Test, **SAET** (Russian Segment thrusters were used for attitude maintenance during test, while US Control Moment Gyros, CMGs, were used before and after it)	0.5 - 1.5
	SAMS2 121f05 at LAB1O1, ER2, Upper Z Panel	Cycle Ergometer with Vibration Isolation System, **CEVIS**	0.1 – 3
	SAMS2 121f03006 at LAB1O1, ER2, Lower Z Panel	**Crew** exercise	< 3
	SAMS2 121f03 at LAB1O1, ER2, Lower Z Panel	Velosiped, **VELO-VB-3M**	2.3, 4.6
	SAMS2 121f03 at LAB1O1, ER2, Lower Z Panel SAMS2 121f05006 at JPM1F5, ER4, Drawer 2	Optimized Propellant Maneuver, **OPM**	0.01 - 6
	MAMS HiRAP at LAB1O2, ER1, Lockers 3,4	**Crew** Glovebox Push-Off *(important for Glovebox data interpretation !!!)*	near 7.5
(*) This band includes the frequency range of the structural modes of the Station. These modes could be excited when short impulsive forces –reboostings- mechanically excite large components of the structure as, for instance, the main Truss and/or the solar panels. Also when different Station maneuvers are effected in order to prepare spacecraft dockings or undockings (for instance, in case of docking, a typical ISS maneuver could start from -XVV/+ZLV TEA attitude to –XVV/+ZLV and back again to -XVV/+ZLV TEA; similarly, an ISS maneuver for undocking could start from +XVV/+ZLV TEA attitude to +ZVV/-XLV and then back again to +XVV/+ZLV TEA).			
(**) 8 < f < 200 Hz	SAMS2 121f02 at LAB1O2, ER1, Drawer 1	Ku-Band Antennas	5 – 20
	SAMS2 121f02 at LAB1O2, ER1, Drawer 1	Russian **SKV** Air Conditioner	23.5
	SAMS2 121f03 at LAB1O1, ER2, Lower Z Panel SAMS2 121f05 at JPM1F5, ER4, Drawer 2	JEM Airlock Vacuum Pump activity	24 (2nd through 4th harmonics) 24 (2nd through 4th harmonics)
	SAMS2 121f02 at LAB1O2, ER1, Drawer 1	Resistive Exercise Device, **RED**	< 30
	MAMS HiRAP at LAB1O2, ER1, Lockers 3,4	Urine Processing Assembly, **UPA**	3.6, 33.3
	SAMS2 121f03 at LAB1O1, ER2, Lower Z Panel	**Robo**naut operations	47.4
	SAMS2 121f04 at LAB1O2, ER1, Lower Z Panel	Internal Thermal Control System, **ITCS**	35 - 60 (also 130, 195)
	SAMS TSH-ES03 at LAB1S2, MSG, Ceiling Plate Y1-B1 Y2-A1	Microgravity Science Glovebox Operations, **MSG**	46 - 47 (normal fans mode) 73 (open fans mode)
	SAMS2 121f02 at LAB1O2, ER1, Drawer 1	Gas Analysis System for Metabolic Analysis of Physiology, **GASMAP**	57 - 58 (fan) 54 - 62 (pumps)
	SAMS2 121f02 at LAB1O2, ER1, Drawer 1	Medical Equipment Computer, **MEC**	59.5 – 70.4
	SAMS2 121f02 at LAB1O2, ER1, Drawer 1	Periodic Fitness Evaluation, **PFE**	68 – 72
	SAMS2 121f05 at JPM1F5, ER4, Drawer 2	**FROST** Stirling Cooler	80
	SAMS2 121f08 at COL1A3, EPM, near PK-4	Centrifuge Rotor of **Biolab**	86.5, 107.3
	SAMS2 121f03 at LABO1, ER2, Lower Z Panel	Station Control Moment Gyroscopes, **CMGs**	110
	SAMS2 121f02 at LAB1S2, MSG, Upper Left Seat Track	General Laboratory Active Cryogenic ISS Experimental Refrigerator, **GLACIER**	60, 120, 180 (Start-up)
	SAMS2 121f08 at COL1A2, ER3, Seat Track near D1	Columbus General Laboratory Active Cryogenic ISS Experimental Refrigerator, **GLACIER-3**	116 - 120 (start-up) near 80 (steady state)
	SAMS2 121f03 at LAB1O1, ER2, Lower Z Panel	Common Cabin Air Assembly, **CCAA**	53 - 128 (inlet variable speed fan) 95 - 100 (water separator fan)
	SAMS2 121f08 at COL1A3, EPM, near PK-4	Electro-Magnetic Levitator, **EML**, in the European Drawer Rack	50 – 90 140 - 170
	SAMS TSH-ES06 at LAB1S4, Fluid Integrated Rack(FIR)	**LAB** Aft Port IMV fan	141.7
	SAMS2 121f04 at LAB1O2, ER1, Lower Z Panel	InterModule Ventilation fans, **IMV**	139 – 145
(**) This band includes the frequency range of the Station internal subsystems, like pumps and fans, used in the different kind of scientific experiments as well as in life support equipment.			